Insight into the factors affecting the reactivity of sulfonic acid species anchored on hyper-cross-linked polymers in esterification

Joanna Wolska [*], Lukasz Wolski

Faculty of Chemistry, Adam Mickiewicz University, Poznań, ul. Uniwersytetu Poznańskiego 8, 61-614 Poznań, Poland

ABSTRACT

The global market for organic esters was estimated at around $89.4 billion in 2022, and is expected to continue to grow, reaching $127.4 billion in 2029. The wide application of mineral acids as homogeneous catalysts for the synthesis of organic esters causes several economic and environmental problems. For this reason, a lot of effort is undertaken to make esterification a more sustainable process. Nowadays, particular attention is paid to the development of new solid acid catalysts containing sulfonic acid groups ($-SO_3H$) supported on organic polymers. This study fits into this scientific trend and aims at providing insight into the factors affecting the reactivity of $-SO_3H$ species anchored on hyper-cross-linked polymers (HCPs). For this purpose, polymers characterized by different cross-linking densities but with a comparable surface area of ca. 540–620 m^2/g and a similar pore size of ca. 3.7 nm were applied as supports for anchoring of $-SO_3H$ through post-synthetic sulfonation. The loading of sulfonic acid species in all prepared catalysts varied from 1.19 to 2.22 mmol/g. Catalytic activity of the sulfonated HCPs (sHCPs) was evaluated in esterification of acetic acid with different alcohols. It was found that the key factors affecting the reactivity of $-SO_3H$ supported on HCPs are hydrophilicity of the polymer surface and the localization of the sulfonic acid species on the external surface of the polymer matrix. The latter was the most favoured during the post-synthetic sulfonation of the polymer characterized by the highest cross-linking density. In the case of this material, the $-SO_3H$ species were approximately 7 times more reactive than those of Amberlyst-15 (TOF = 11.36 vs. 1.57 h^{-1}, respectively). The most efficient sHCP used in this study reached approximately two times higher conversion of *n*-butanol than Amberlyst-15 (53.6 vs. 27.5 %) despite of the significantly lower loading of sulfonic acid species in the former polymer (2.22 vs. 4.66 mmol/g, respectively). It was also established that the catalytic esterification on the surface of sHCPs proceeded according to the Langmuir-Hinshelwood mechanism, in which chemisorption of the alcohol is the rate-determining step. Moreover, sHCP catalysts could be reused four times without significant deactivation.

1. Introduction

The esterification reaction of carboxylic acid with an alcohol is one of the most important groups of liquid-phase organic transformations (Khan et al., 2021). The resulting esters belong to valuable fine chemicals widely used in the manufacturing of paints (Mirabedini et al., 2020), varnishes (Benessere et al., 2019), perfumes (Sá et al., 2017), coatings (Wang et al., 2020), pharmaceuticals (Arca et al., 2018) and even cosmetics (Khan and Rathod, 2015). Esters also play an important role in the field of the petrochemical industry, being one of the main components of biodiesel (Ambat et al., 2018; Mohamed et al., 2023). According to a very recent report by Future Market Insights, the global esters market was estimated at around $89.4 billion in 2022, and is

expected to continue to grow, reaching $127.4 billion in 2029 (https://www.futuremarketinsights.com/reports/esters-market.).

The esterification reaction can be efficiently catalyzed by mineral acids such as sulfuric, hydrochloric, hydroiodic or *para*-toluenesulfonic acids (Khan et al., 2021). These homogeneous catalysts are relatively inexpensive and exhibit good catalytic activity. However, one of the most important drawbacks of their use are corrosion of the equipment, the formation of acidic waste and the difficulties in recovery and reuse of the catalysts. Such obstacles are the major impetus for the development of alternative and more environmentally benign heterogeneous catalysts to make esterification a more sustainable process. To date, various inorganic and organic nanomaterials such as zeolites (Li et al., 2023; Zhang et al., 2014; Prinsen et al., 2018; Gomes et al., 2022), organic ion-

exchange resins (Bringué et al., 2019; Reinoso and Boldrini, 2020; Di Menno Di et al., 2022), metal–organic frameworks (MOFs) (Yılmaz et al., 2017; Zang et al., 2013), or supported heteropoly acids (Desai and Yadav, 2023; Paiva et al., 2022) have been recognized as promising substitutes for the homogeneous catalysts based on mineral acids. Nevertheless, large-scale application of the above-mentioned nanomaterials is still limited because of their important drawbacks. For example, it is very often that microporous structure of zeolites causes difficulties with the availability of the active sites to the reagents and results in mass transfer limitations (Liu et al., 2022). On the other hand, the reactivity of strongly acidic ion-exchange resins such as Amberlyst® or Dow® is usually reduced by their relatively low specific surface area (Kim et al., 2020). Additionally, most of MOFs suffer from low thermal stability that often disqualifies them as effective SACs (Healy et al., 2020). In view of these problems, researchers are still undertaking a lot of effort to find the more efficient solid acid catalysts (SACs).

Hyper-cross-linked polymers (HCPs) are classified as porous organic polymers (POPs) and possess several desirable features for their application as promising supports for heterogeneous catalysts dedicated to esterification. HCPs have a relatively large surface area (more than 1000 m^2/g (Woodward, 2020)), as well as high mechanical and thermochemical stabilities (Tan and Tan, 2017). Moreover, they can be easily synthesized by a facile, inexpensive, and scalable method based on Friedel-Crafts alkylation (Li et al., 2011). Due to their unique physicochemical properties, HCP-based materials have been successfully used as highly efficient adsorbents for wastewater remediation, e.g. (Hamza et al., 2021; Wei et al., 2021; He et al., 2021). Concerning the application of HCPs-based polymers as catalysts for the esterification reaction, data from the recent literature show that current studies in this field focus primarily on i) the development of novel SACs by searching for a new building blocks and/or cross-linking agents that could lead to the obtainment of more desirable properties of these organic supports, and ii) the evaluation of the reactivity of synthesized nanomaterials (Kalla et al., 2018; Bhunia et al., 2015; Zheng et al., 2013; Kundu and Bhaumik, 2015; Munyentwali et al., 2021). For example, Munyentwali *et al.* (Munyentwali et al., 2021) synthesized a series of 1,3,5-tri(4-vinyl-phenyl)-benzene- and divinylbenzene-based sulfonated HCPs (sHCPs) containing a similar amount of sulfonic acid species (from 2.2 to 2.3 mmol/g) but characterized by totally different surface area and hydrophobicity. They revealed that the higher the hydrophobicity of the polymer surface, the higher the catalytic activity in the esterification reaction of fatty acids with methanol. However, in addition to differences in the hydrophilicity of the polymers, the examined sHCPs also had totally different BET surface areas ranging from 478 to 738 m^2/g for the most hydrophilic and hydrophobic polymers, respectively. Thus, one can expect that the improved reactivity of the most hydrophobic material could also result, to some extent, from its much higher surface area that enabled better accessibility of the surface active sites to the reagents. Further, the undeniable significance of a compromise between hydrophobicity and acidity of the polymer matrix was also recently reported by Blocher *et al.* (Blocher et al., 2022). The authors synthesized a series of 4,4′-bis-(chloromethyl)biphenyl-based sulfonated HCPs containing different amounts of sulfonic acid sites (0.03–3.76 mmol/g), and tested their activity in the hydrolysis of cyclohexyl acetate. The highest activity was observed for the polymer containing 2.2 mmol/g of −SO$_3$H groups. A higher loading of acid sites (above 2.2 mmol/g) resulted in decreased catalyst activity. According to the authors, the highest activity of sHCP containing 2.2 mmol/g of −SO$_3$H originated from the most suitable compromise between several features of this material, including: porosity, surface area, amphiphilicity, and surface acidity. However, a clear conclusion about the role of the individual factors in controlling the reactivity of sHCPs was difficult to estimate because of the multiple variations in the physicochemical properties of the investigated catalysts. Based on above, one can clearly conclude that fundamental studies aiming at evaluation of the relationship between the cross-linking density of HCPs, and their physicochemical and surface

properties as well as catalytic activity in esterification are sparse.

This study aims at filling this gap in the fundamental knowledge mentioned above by providing deep insight into the factors affecting the reactivity of sulfonated hyper-cross-linked polymers, based on triphenylmethane (TPM) as an aromatic building block and formaldehyde dimethyl acetal (FDA) as an external cross-linking agent, in esterification of acetic acid with selected aromatic and aliphatic alcohols. The HCP-based polymers used in this study were characterized in detail in our previous article related to the adsorptive removal of antibiotic pollutants from water (Wolska et al., 2023). They had similar porosity and surface area, and differed only in terms of hydrophilicity/hydrophobicity of their surfaces, which originated from various localization and loading of sulfonic acid species in the polymer matrix. Based on the above information, one can conclude that the physicochemical properties of these organic polymers make them very promising model catalysts for assessing the role of surface hydrophilicity/hydrophobicity as well as localization and loading of −SO$_3$H species in controlling the reactivity of these surface active sites in esterification. As described above, the majority of previous fundamental studies in this field have been performed using nanomaterials that differ significantly both in terms of their textural/structural properties and sulfur content, which hindered the unambiguous analysis of the experimental data. Catalytic activity of the sulfonated polymers used in this study was evaluated in esterification of acetic acid with different structure alcohols (methanol, *n*-butanol, cyclohexanol and benzyl alcohol) yielding esters of high industrial significance. The reactivity of the polymers was also compared with that established for commercial Amberlyst-15, which is known as efficient SAC and is usually used as reference material (Taddeo et al., 2022; Hykkerud and Marchetti, 2016; Melfi et al., 2020). A significant part of this work also covered analysis of the mechanism of the esterification process on the surface of sulfonated HCPs.

2. Experimental methods

2.1. Chemicals and reagents

The chemicals and reagents used in this study were the following: methanol (MeOH, Sigma-Aldrich, 99.8 %), *n*-butanol (*n*-BuOH, Sigma-Aldrich, ≥ 99.4 %), cyclohexanol (CyOH, Sigma-Aldrich, 99.0 %), benzyl alcohol (BnOH, Sigma-Aldrich, anhydrous, 99.8 %), acetic acid (AcH, Sigma-Aldrich, 99–100 %), sodium hydroxide (NaOH, POCH, 98.8 %), phenolphthalein (Sigma-Aldrich, ACS reagent), ethanol (EtOH, STANLAB, 99.9 %), oxalic acid (Sigma-Aldrich, ≥ 99 %). Commercial ion-exchange organic resin (Amberlyst-15, hydrogen form, Sigma-Aldrich) was used as reference material. All chemicals were used as received. Deionized water was used throughout the experiments.

2.2. Catalyst preparation

The pristine triphenylmethane-based hyper-cross-linked polymers (HCP1, HCP2, and HCP3) characterized by different cross-linking density were prepared by the Friedel-Crafts knitting using different molar ratio between the aromatic building block (triphenylmethane, TPM) and the external cross-linking agent (formaldehyde dimethyl acetal, FDA) (TPM/FDA molar ratio of 1.0/4.5, 1.0/9.0 and 1.0/13.5 for HCP1, HCP2, and HCP3, respectively). Sulfonic acid groups were anchored on the polymer matrix by post-synthetic sulfonation using chlorosulfonic acid (ClSO$_3$H) as a sulfonating agent. The resulting sulfonated HCPs were labeled as sHCP1, sHCP2, and sHCP3. Experimental details related to the synthesis of all HCP-based materials are described in an extended experimental section (see Supporting Information).

2.3. Characterization of materials

Experimental details related to the analysis of chemical composition, structure, and texture parameters of all HCPs-based catalysts used in this

study, as well as their wettability properties (by water contact angle measurements) and ion exchange capacity are described in the extended experimental section (see Supporting Information).

2.4. Catalytic tests

All catalytic tests were performed in a round-bottom flask equipped with a condenser. The catalysts were tested in the esterification of acetic acid (AcH) with four different structure alcohols (methanol, *n*-butanol, cyclohexanol, or benzyl alcohol) (Scheme 1). In a typical experiment, 20 mg of the HCP-based catalyst (dried overnight at 80 °C under vacuum) were added to the mixture of AcH (1.0 eq., 64.0 mmol) and the corresponding alcohol (2.0 eq., 128.0 mmol) under vigorous stirring (400 rpm). All reactions were carried out at 100 °C, with the exception of the reaction with MeOH, which was carried out at 50 °C, due to the lower boiling temperature of the alcohol and the resulting methyl acetate (57–58 °C (Pöpken et al., 2001)). After a given reaction time (*t*), the conversion of the AcH was estimated by acid-base titration method with 0.1 M NaOH aqueous standard solution using phenolphthalein as an indicator. For this purpose, aliquots were collected into a syringe and the catalyst was separated from the solution by filtration through a 0.2 µm syringe filter (PTFE, Lab Logistics). The syringe filter was conditioned by washing with a small portion of the previously collected solution. The conversion of AcH to the corresponding acetate ester (methyl acetate, *n*-butyl acetate, cyclohexyl acetate, or benzyl acetate) as the only product of this esterification was calculated using equations (Eqs. S2-S3, see Supporting Information). All catalytic tests were performed at least three times under given reaction conditions. The values presented in the article are mean values of the AcH conversion. Pre-adsorption experiments were carried out by pre-mixing sHCP1 with AcH and/or *n*-BuOH at room temperature for 24 h followed by heating to 100 °C and adding the remaining reagent. To exclude possible diffusion limitation effects (external mass transfer resistance) during the catalytic tests, a series of experiments at different stirring rates were performed (Fig. S1). According to the results, increasing the stirring rate from 150 to 400 rpm resulted in a slight increase in the AcH conversion. However, a further increase in the stirring rate to 700 rpm did not have a significant influence on the conversion of acetic acid. This means that the effect of external mass transfer resistance was eliminated when a stirring rate of 400 rpm was applied. A similar phenomenon was also reported in

previous studies (Abbas et al., 2016). To avoid the potential impact of the diffusion limitations on AcH conversion, all catalytic tests were carried out using a stirring rate of 400 rpm.

2.5. Reuse experiments

In a typical reuse experiment, 30 mg of sHCP1 (dried overnight at 80 °C under vacuum) were added to the mixture of AcH (1.0 eq., 64.0 mmol) and *n*-BuOH (2.0 eq., 128.0 mmol) under vigorous stirring (400 rpm). The reaction was carried out at 100 °C for 240 min. After this time, the sHCP1 catalyst was separated from the reaction mixture through PTFE filter paper (Ahlstrom, 0.45 µm) on a glass vacuum filtration apparatus (Glassco). The conversion of AcH was estimated by the acid-base titration method with aqueous standard solution of 0.1 M NaOH using phenolphthalein as an indicator. The spent sHCP1 catalyst was washed with 50 mL of acetone and dried at 80 °C for 18 h before the next reaction cycle. The regeneration performance of sHCP1 was studied in a total of four reaction cycles.

In order to evaluate the stability of the sHCP1 catalyst, the material after the forth reaction cycle was subjected to ATR-IR, XPS and elemental analyses. Before all measurements, the spent sHCP1 sample was dried under vacuum at 80 °C for 24 h. The infrared spectra of the spent sHCP1 polymer were acquired using a Bruker Vertex 70 spectrophotometer equipped with an platinum attenuated total reflectance (ATR) accessory (Bruker). X-ray photoelectron spectroscopy (XPS) was performed using an ultra-high vacuum photoelectron spectrometer based on a Phoibos150 NAP analyzer (Specs, Germany). The analysis chamber was operated under vacuum with a pressure close to 5×10^{-9} mbar and the sample was irradiated with monochromatic AlKα (1486.6 eV) radiation. Any charging that might occur during the measurements (due to incomplete neutralization of ejected surface electrons) was accounted for by rigidly shifting the entire spectrum by a distance needed to set the binding energy of the C 1 s assigned to adventitious carbon to the assumed value of 284.8 eV. Elemental analysis (EA) of the spent sHCP1 catalyst was carried out with an Elementar Analyser Vario EL III. The polymer was weighed in tin capsules (catalyst mass: 4 mg) and introduced into the reactor with a precisely defined portion of oxygen. After combustion at 900–1000 °C, the exhaust gases were transported in helium flow to the second reactor, and then through the water trap to the chromatographic column, which separated the generated
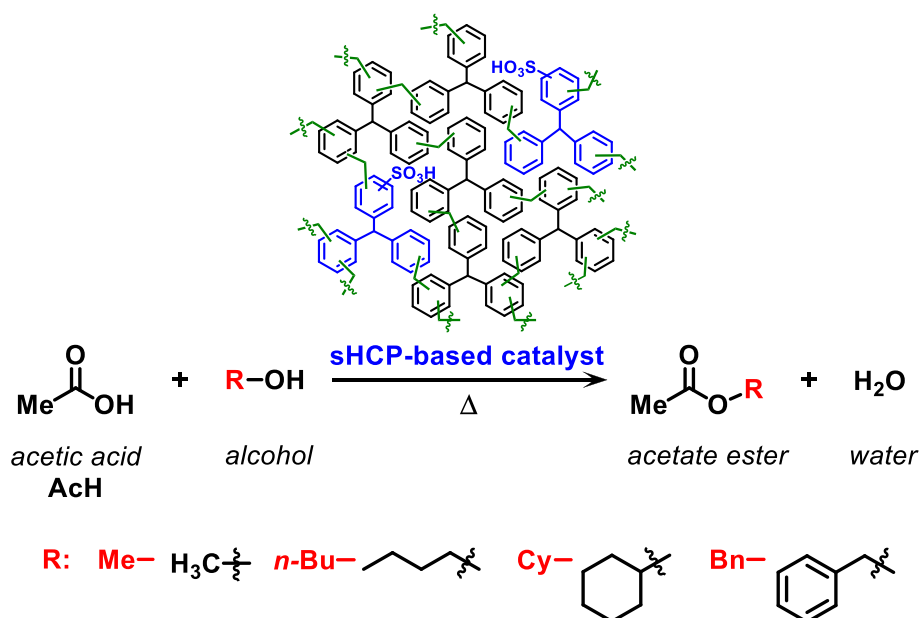
Scheme 1. Esterification of acetic acid (AcH) and different structure alcohols (methanol, MeOH; *n*-butanol, *n*-BuOH; cyclohexanol, CyOH; or benzyl alcohol, BnOH) with the use of sHCP-based solid acid catalysts.

gases. Finally, the separated gases were detected by a thermal conduction detector (TCD). The measurements were repeated three times for each investigated sample.

3. Results and discussion

3.1. Physicochemical characteristics of the polymers

Table 1 presents the most important physicochemical properties of the polymers used in this study. All sulfonated HCPs have a comparable surface area of 538–628 m^2/g and a similar average pore size of 3.72 nm, but differ slightly in terms of sulfur content. The highest sulfur loading was observed for the material characterized by the lowest cross-linking density (sHCP1). The higher the cross-linking density, the lower the efficiency of sulfur anchoring during the post-synthetic sulfonation process. In the case of the polymer with the highest cross-linking density (sHCP3), the sulfur content was approximately two times lower than that established for sHCP1 (1.19 vs. 2.22 mmol/g, Table 1). In all polymers used in this study, sulfur existed only in the form of –SO₃H species (for more details please see the XPS and FTIR sections in our previous work (Wolska et al., 2023). As implied by the data from Table 1, good agreement was observed between the sulfur content determined by elemental analysis and acid-base titration, indicating that all sulfonic acid species anchored on the polymers were available for reagents. Slightly higher values obtained during the estimation of acid exchange capacity using the acid-base titration method resulted more likely from the presence of some side products of Friedel-Crafts alkylation which are usually formed during the knitting process (e.g. –CH₂OH groups (Paul et al., 2020)). In all pristine HCPs the content of these side products was similar (0.19 mmol/g) and much lower than the sulfur loading. A more detailed description of the morphology, structure, and physicochemical properties of the polymers is provided in our previous article (Wolska et al., 2023).

3.2. Activity of polymer-based catalysts in esterification

Fig. 1 shows the catalytic activity of polymer-based materials used in this study in esterification of acetic acid with *n*-butanol. Conversion of acetic acid in the presence of pristine HCPs supports was only slightly higher than that established for the reaction without catalyst (ca. 10 vs. 6 %, respectively; Fig. 1). This showed that the polymeric matrixes themselves exhibited negligible activity in esterification. The anchoring of the sulfonic acid groups on HCP-based materials resulted in a significant increase in their activity, indicating that the –SO₃H species were the key active species in this reaction. The highest acetic acid conversion was observed for the reaction with the use of sHCP1, which possesses the highest –SO₃H loading. This catalyst enabled an approximately two times higher conversion of acetic acid than that observed for the commercial Amberlyst-15, which contained a much larger amount of sulfonic acid species than sHCP1 (Fig. 1 and Table 1). As far as sulfur content is concerned, it is important to underline that sHCP1 contained approximately 2 times more sulfur than sHCP3 (2.22 vs. 1.19 mmol/g, respectively; Table 1), but the reactivity of the former catalyst was only slightly higher than the latter (53.6 vs. 44.1 % of AcH conversion, respectively; Fig. 1). Moreover, sHCP2 and sHCP3 exhibited comparable acetic acid conversion (44.7 vs. 44.1 %, respectively; Fig. 1) despite of the fact that these polymers had different sulfur content (Table 1). All of these observations allowed for the conclusion that the reactivity of sulfonic acid species anchored on hyper-cross-linked polymers may be somehow related to the surface properties of the polymeric supports.

To shed more light on the reactivity of a single sulfonic acid site in esterification, TOF values were calculated. As implied by the data shown in Table 2, the highest TOF value was observed for –SO₃H species anchored on the surface of the hyper-cross-linked polymer characterized by the highest cross-linking density (sHCP3). The lower the cross-linking density of the polymer matrix, the lower the reactivity of a single sulfonic acid site in esterification (Table 2).

A similar relationship between the reactivity of a single –SO₃H site in sHCPs and the cross-linking density of the polymer matrix was also observed for the esterification of other alcohols, including: methanol, cyclohexanol, and benzyl alcohol (Table 2). In all these reactions, the
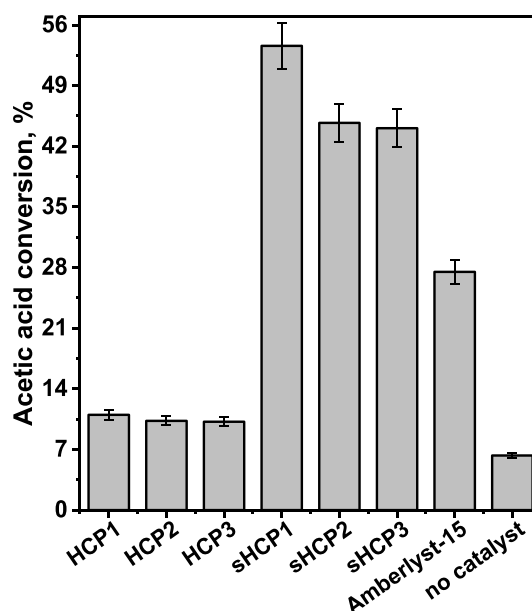
Table 1
Textural parameters, contact angle values, sulfur content, and acid exchange capacity of all investigated catalysts [Reprinted from (Wolska et al., 2023), Copyright (2023), with permission from Elsevier].

Catalyst	S_{BET}[a] $[m^2/g]$	Average pore diameter[b] [nm]	CA[c] [°]	Sulfur content[d] [mmol/g]	Acid exchange capacity[e] [mmol/g]
sHCP1	628	3.72	47 ± 0.1	2.22 ± 0.03	2.71 ± 0.13
sHCP2	538	3.72	45 ± 0.1	1.48 ± 0.02	1.59 ± 0.07
sHCP3	540	3.72	43 ± 0.1	1.19 ± 0.02	1.46 ± 0.06
HCP1	1061	3.72	50 ± 0.1	n/a	0.19
HCP2	910	3.72	53 ± 0.1	n/a	0.19
HCP3	939	3.94	58 ± 0.1	n/a	0.19
Amberlyst-15	43[f]	n/a	n/a	4.66 ± 0.07	4.65 ± 0.23

[a] Specific surface area calculated using the BET model;
[b] Average pore diameter calculated from the desorption branch of the isotherms using the Barrett-Joyner-Halenda (BJH) method;
[d] Average values derived from three measurements determined based on EA;
[c] Water contact angle derived from three to five measurements;
[e] Average values derived from three measurements determined based on the acid-base titration method (see Eq. S9);
[f] BET surface area from reference no. (Kim et al., 2020).

Fig. 1. Conversion of acetic acid in esterification of acetic acid with *n*-butanol in the presence of pristine and sulfonated HCPs as catalysts. Amberlyst-15 was used as the reference material. *Reaction conditions*: AcH (3.84 g, 3.66 mL, 1.0 equiv., 64.0 mmol), *n*-BuOH (9.49 g, 11.71 mL, 2.0 equiv., 128.0 mmol), 20 mg of catalyst (excluding blank trial), 400 rpm, 100 °C, 120 min.

Table 2

Conversion of acetic acid and TOF values calculated for the esterification of acetic acid with different alcohols on a series of sHCPs (sHCP1-sHCP3) and Amberlyst-15.

Catalyst	MeOH[a]		BnOH[b]		n-BuOH[c]		CyOH[d]	
	Conv.[e] [%]	TOF[f] [h^{-1}]	Conv.[e] [%]	TOF[f] [h^{-1}]	Conv.[e] [%]	TOF[f] [h^{-1}]	Conv.[e] [%]	TOF[f] [h^{-1}]
sHCP1	41.5	2.49	57.6	3.46	32.4	7.79	24.2	1.45
sHCP2	33.7	2.93	55.9	4.87	25.2	8.78	22.9	1.99
sHCP3	29.1	3.27	55.0	6.18	25.3	11.36	22.3	2.50
Amberlyst-15	30.1	0.86	55.2	1.58	27.5	1.57	13.4	0.38

[a] *Reaction conditions:* AcH (3.84 g, 3.66 mL, 1.0 equiv., 64.0 mmol), MeOH (4.10 g, 5.18 mL, 2.0 equiv., 128.0 mmol), 20 mg of catalyst, 400 rpm, 50 °C, 240 min;
[b] *Reaction conditions:* AcH (3.84 g, 3.66 mL, 1.0 equiv., 64.0 mmol), BnOH (13.84 g, 13.25 mL, 2.0 equiv., 128.0 mmol), 20 mg of catalyst, 400 rpm, 100 °C, 240 min;
[c] *Reaction conditions:* AcH (3.84 g, 3.66 mL, 1.0 equiv., 64.0 mmol), n-BuOH (9.49 g, 11.71 mL, 2.0 equiv., 128.0 mmol), 20 mg of catalyst, 400 rpm, 100 °C, 60 min;
[d] *Reaction conditions:* AcH (3.84 g, 3.66 mL, 1.0 equiv., 64.0 mmol), CyOH (12.82 g, 13.52 mL, 2.0 equiv., 128.0 mmol), 20 mg of catalyst, 400 rpm, 100 °C, 240 min;
[e] The conversion of AcH was calculated using equations (Supplementary Information Eqs. S2-S3);
[f] TOF was calculated as moles of AcH converted over 1 mol of sulfonic acid sites (determined by acid-base titration method) per 1 h (Supplementary Information, Eqs. S4-S8).

AcH conversion and TOF values calculated for the catalysts based on sulfonated hyper-cross-linked polymers were significantly higher than those established for Amberlyst-15 (Table 2). The most pronounced difference in reactivity of a single $-SO_3H$ site anchored on the HCPs characterized by the highest cross-linking density and Amberlyst-15 was observed for the esterification of acetic acid with n-butanol and cyclohexanol (approximately 7 times higher TOF for sHCP3 than for Amberlyst-15; Table 2). In the case of methanol and benzyl alcohol, the differences in TOF values for these two catalysts were less pronounced, but the sulfonic acid species anchored on the HCPs were still more reactive than those in Amberlyst-15. This phenomenon will be discussed in the later part of the article (see Section 3.3).

The most active polymer (sHCP1) that enabled the highest acetic acid conversion after 120 min of the reaction was used for optimization studies aiming to elucidate the impact of reaction temperature, time, and catalyst loading on the esterification efficiency. As shown in Fig. 2, the reaction temperature had a significant impact on the reactivity of the catalyst. At 50 °C, sHCP1 exhibited very low activity, reaching only 8.7 % of acetic acid conversion after 120 min. The increase in temperature to 75 °C allowed for a noticeable increase in AcH conversion from 8.7 % at 50 °C to 36.2 % at 75 °C. The highest activity of the catalyst was observed at 100 °C (approximately 70 % of the AcH conversion). As shown in Fig. 2, a further increase in the reaction temperature to 110 °C

did not result in a noticeable increase in the conversion of n-butanol. Thus, the results obtained in this study clearly showed that the activity of sHCP1 in esterification of acetic acid with n-butanol is almost directly proportional to the reaction temperature when the temperature varies from 50 to 100 °C (Fig. 2), and the optimal temperature for the most efficient conversion of AcH is 100 °C. Furthermore, these results clearly indicate that the efficiency of esterification reaction in the presence of the sHCP1 catalyst can be simply tuned by controlling the temperature.

Less pronounced differences in the reactivity of sHCP1 were observed by changing the catalyst loading. As shown in Fig. 3, sHCP1 exhibited high AcH conversion even at very low catalyst loading of 0.07 wt%. Increasing the catalyst loading to 0.15 wt% resulted in a noticeable increase in AcH conversion, but the difference was not as significant as in the case of assessing the effect of reaction temperature. When the catalyst loading was tripled (from 0.07 to 0.22 wt%), the conversion of acetic acid increased only by approximately 15 % (Fig. 3). Similar observations related to the slight effect of catalyst dosage on the enhancement of esterification efficiency were also reported in previous studies (Bhorodwaj and Dutta, 2011; Pan et al., 2013). As far as the impact of catalyst loading is concerned, it is important to underline that the esterification reaction can be efficiently catalyzed using a very small amount of the sHCP1 catalyst (0.07 wt%). When compared with other results in this field, such low catalyst loading was rarely used in
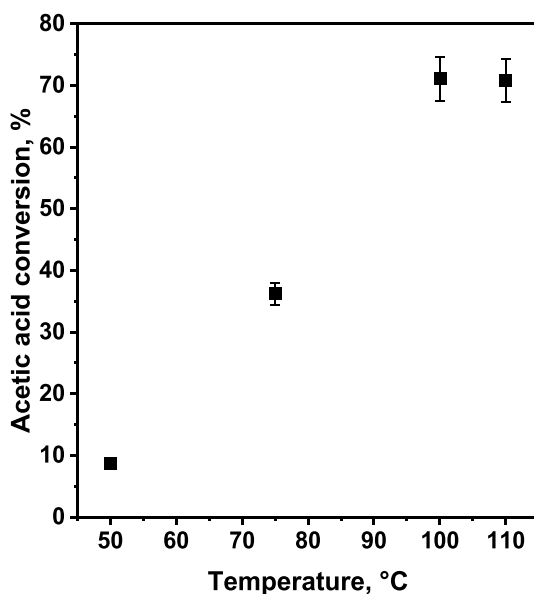

Fig. 2. The influence of temperature on the conversion of acetic acid in esterification of acetic acid with n-butanol in the presence of sHCP1 catalyst. *Reaction conditions*: AcH (3.84 g, 3.66 mL, 1.0 equiv., 64.0 mmol), n-BuOH (9.49 g, 11.71 mL, 2.0 equiv., 128.0 mmol), 20 mg of sHCP1, 400 rpm, 240 min.
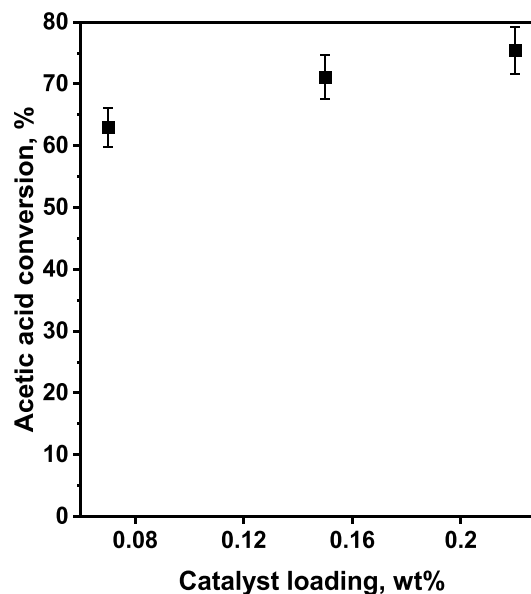

Fig. 3. The influence of the sHCP1 loading on acetic acid conversion in esterification of acetic acid with n-butanol. *Reaction conditions*: AcH (3.84 g, 3.66 mL, 1.0 equiv., 64.0 mmol), n-BuOH (9.49 g, 11.71 mL, 2.0 equiv., 128.0 mmol), 400 rpm, 100 °C, 240 min.

esterification reaction (see Table S1). Usually, a much higher dose of catalyst (up to 2 wt%) was applied to achieve a similar conversion of the acetic acid (Yılmaz et al., 2017; Zang et al., 2013; Masteri-Farahani and Shahsavarifar, 2021; Wolska et al., 2021; Hosseini and Masteri-Farahani, 2019).

Regarding the effect of the reaction time, it was observed that the conversion of acetic acid increased as the reaction time was prolonged (Fig. 4). The highest rate of the reaction was observed at the beginning of the esterification (up to 120 min), but after a longer time the rate of the esterification became slower and the changes in AcH conversion were significantly less pronounced. However, approximately 85 % of the acetic acid conversion has been observed after 960 min (16 h), indicating that sHCP1 can efficiently catalyze the esterification reaction reaching very high AcH conversion even at low catalyst loading. A similar relationship between the reaction time and the rate of the esterification reaction was observed in many previous studies (Liu et al., 2006; Pirez et al., 2012; Hu et al., 2020), and is related to the reduction of the reaction rate when approaching the equilibrium state (usually approximately 80–90 % of the AcH conversion, depending on the reaction conditions (Bhorodwaj and Dutta, 2011; Miao and Shanks, 2011). This effect is most probably associated with the inhibiting effect of the water that is formed as a side product of esterification (Liu et al., 2006).

The most active sHCP1 polymer was also subjected to stability tests in four subsequent reaction cycles. As shown in Fig. 5, a slight decrease in AcH conversion was observed from 73.7 % during the first cycle to 62.8 % in the second cycle. Slightly decreasing activity was also observed in the third reaction cycle, but the drop in AcH conversion was much less pronounced than that observed in the second cycle. Interestingly, in a fourth reaction cycle AcH conversion was similar to that of the third cycle, indicating that there was no further noticeable decrease in the catalytic activity of the sHCP1 catalyst. Thus, after four reaction cycles the AcH conversion decreased only by ca. 15 %, indicating relatively high stability and reusability of sHCP1 polymer. Detailed characterization of the spent polymer after four reaction cycles led us to establish the origin of catalyst deactivation. As shown in Fig. S2, there were no significant differences in the structure of the fresh sHCP1 catalyst and the material after four reuse tests. The IR spectra of these two samples were the same, and all vibrational bands typical of the polymer matrix and the sulfonic acid species were preserved. For
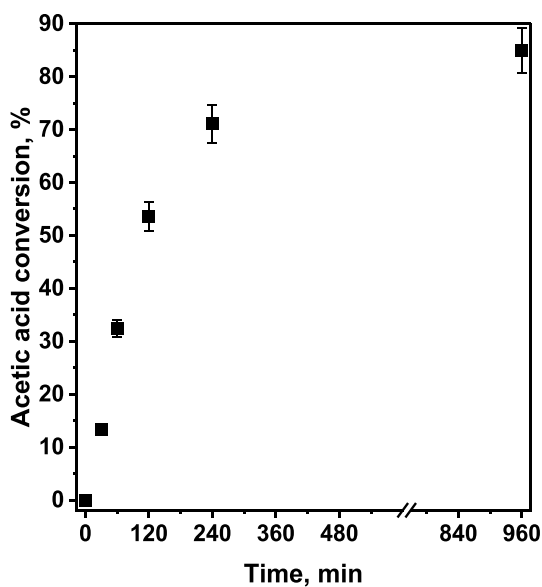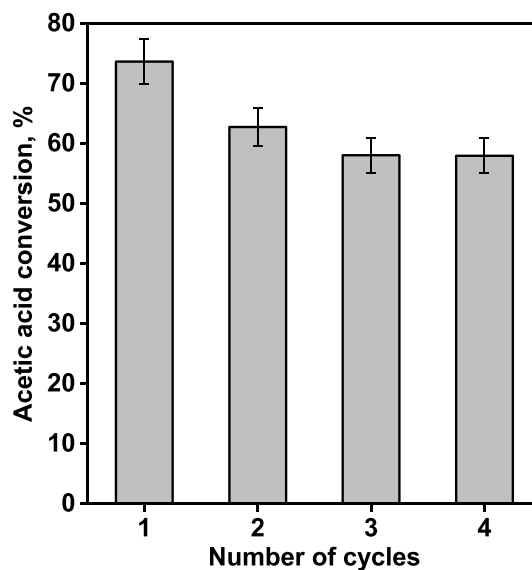

Fig. 5. Stability of the sHCP1 catalyst during four reaction cycles. *Reaction conditions*: AcH (3.84 g, 3.66 mL, 1.0 equiv., 64.0 mmol), *n*-BuOH (9.49 g, 11.71 mL, 2.0 equiv., 128.0 mmol), 30 mg of catalyst, 400 rpm, 100 °C, 240 min. Details related to the reuse tests are described in the experimental section.

example, the IR spectrum of the recycled sHCP1 catalyst revealed the presence of a broad absorption band between 3680 and 3100 cm^{-1} that is assigned to the stretching vibration of the O−H bonds in −SO$_3$H groups (Fig. S2, region a) (Giri et al., 2022). Furthermore, the chemical stability of the reused sHCP1 catalyst was also confirmed by the preservation of IR bands at approximately 1225–1175 cm^{-1} and 1080–1020 cm^{-1}, which are attributed to asymmetric and symmetric stretching vibrations of the S=O bonds in sulfonic acid species, respectively (Zhang et al., 2023). The presence of −SO$_3$H species on the surface of the reused sHCP1 polymer was also confirmed by XPS measurements. As shown in Fig. S3, no significant changes in the S 2p binding energy region were noticed, indicating that the active sites remained unchanged after four reaction cycles. On the basis of the above data, one can clearly conclude that the decrease in catalyst activity during the first two reaction cycles could not be related to changes in the structure of the sHCP1 polymer and/or nature of the active sites. According to the literature (Zhao et al., 2023; Yahya and Elshaarawy, 2023), the deactivation of sulfonated polymers may also originate from leaching phenomena. To verify a possible contribution of this effect to the deactivation of the sHCP1 polymer, the chemical composition of the reused catalyst was determined by elemental analysis. As implied by Table S2 data, the loading of −SO$_3$H species in the sHCP1 polymer decreased from 2.22 to 1.76 mmol/g after four reaction cycles. This observation led us to clearly indicate that the main factor contributing to the decreasing activity of the sHCP1 polymer is leaching of the active species. Since changes in catalyst activity during the third and fourth reaction cycles were much less pronounced in comparison with those observed during the first two reaction cycles, we claimed that the leaching phenomena took place mainly during the first two reaction cycles. Similar conclusions related to the stability and reusability of sulfonated polymers were also reported in our previous studies (Wolska et al., 2021), and other data from the literature (e.g. (Zhao et al., 2023; Yahya and Elshaarawy, 2023)).

3.3. Discussion

The results obtained in this study clearly show that the reactivity of a single sulfonic acid site in esterification reaction is somehow related to the composition/surface properties of hyper-cross-linked polymers. The highest TOF values were observed for sHCP3, which is characterized by the highest cross-linking density and the lowest sulfur loading. Since all

Fig. 4. Conversion of acetic acid in esterification of acetic acid with *n*-butanol as a function of reaction time in the presence of sHCP1 catalyst. *Reaction conditions*: AcH (3.84 g, 3.66 mL, 1.0 equiv., 64 mmol), *n*-BuOH (9.49 g, 11.71 mL, 2.0 equiv., 128 mmol), 20 mg of sHCP1, 400 rpm, 100 °C.

polymers used in this study have similar surface area and porosity (Table 1), the contribution of these two features to the enhancement of –SO₃H reactivity by improving the availability of the active sites to the reagents could be omitted. According to the literature (Zhang et al., 2014; Manjunathan et al., 2021), other factors that can have a significant impact on the reactivity of sulfonic acid species anchored on polymeric supports are the strength of the acid sites and the hydrophilicity of the polymer matrix. Both of these factors are strongly affected by the –SO₃H loading and increase with increased sulfur content (Manjunathan et al., 2021). As concerns the former factor, it was established that the lower the strength of –SO₃H groups anchored on a polystyrene-based supports, the higher their reactivity in esterification (Zhang et al., 2014). Thus, the lowest reactivity of the –SO₃H species anchored on sHCP1 could be explained by the highest strength of the acid sites in this polymer. However, significant differences in TOF values for sHCP2 and sHCP3 which have similar –SO₃H loading clearly indicate that the strongly enhanced reactivity of sHCP3 cannot be attributed solely to the different strength of the acid sites. This implies that the mentioned above differences in reactivity of a single sulfonic acid site on the surface of the polymers used in this study may be significantly affected by the hydrophilicity/hydrophobicity of the polymer matrix. To shed more light on the possible contribution of the latter factor to the enhancement of –SO₃H reactivity, we attempted to clarify the esterification mechanism. According to previous studies, the esterification reaction catalyzed by SACs most often involves the adsorption of one or two surface-bound species corresponding to an Eley-Rideal or Langmuir-Hinshelwood type mechanism, respectively (Zeng et al., 2012; Mitran et al., 2015). For example, Altıokka and Çand et al. (Altıokka and Çıtak, 2003) reported that esterification of acetic acid and isobutanol over the commercial Amberlite IR-120 catalyst followed the former mechanism (Eley-Rideal) in which alcohol is chemisorbed on the catalyst surface (the rate-determining step) and reacts with acetic acid from the liquid (bulk) phase. On the other hand, Lee et al. (Lee et al., 2002) demonstrated that esterification of propionic acid with n-butanol over Amberlyst 35 followed the latter mechanism (Langmuir-Hinshelwood) in which both substrates need to be adsorbed on ion-exchange resin to proceed the reaction. To clarify the mechanism of esterification of n-butanol over sulfonated HCP-based polymers, we performed additional catalytic tests preceded by pre-adsorption of selected reagents (Mitran et al., 2015). In our studies we considered three different scenarios: i) pre-adsorption of n-butanol at room temperature for 24 h followed by heating to 100 °C and initiation of the reaction by addition of acetic acid, ii) pre-adsorption of acetic acid at room temperature for 24 h followed by heating to 100 °C and initiation of the reaction by addition of n-butanol, and iii) pre-adsorption of both acetic acid and n-butanol at room temperature for 24 h followed by heating to 100 °C. The results obtained from the pre-adsorption tests were compared with those in which the pre-adsorption step was very short (5 min). Please note that such a short pre-adsorption step and the order of the reagents mixing have negligible influence on the efficiency of the esterification reaction (Fig. S4). According to the results, long pre-adsorption of acetic acid did not affect the AcH conversion (Fig. 6). On the other hand, pre-adsorption of n-BuOH for 24 h resulted in a significant increase in AcH conversion (Fig. 6). Interestingly, when both reagents were pre-adsorbed on the sHCP1 catalyst for a long time, the conversion of acetic acid was the same as for the experiment without pre-adsorption of any reagent and with pre-adsorption of AcH only.

In view of these results, one can clearly conclude that the rate-determining step of the overall esterification reaction over sHCPs is the chemisorption of the alcohol on the polymer surface. Moreover, results obtained by pre-adsorption of both reagents clearly showed that acetic acid has a higher affinity to the catalyst surface than n-butanol, and chemisorption of the carboxylic acid limits the efficiency of the alcohol chemisorption. Since chemisorption of acetic acid on the catalyst surface hinders availability of the active sites for activating alcohol, and alcohol chemisorption is the rate-determining step, we claimed that
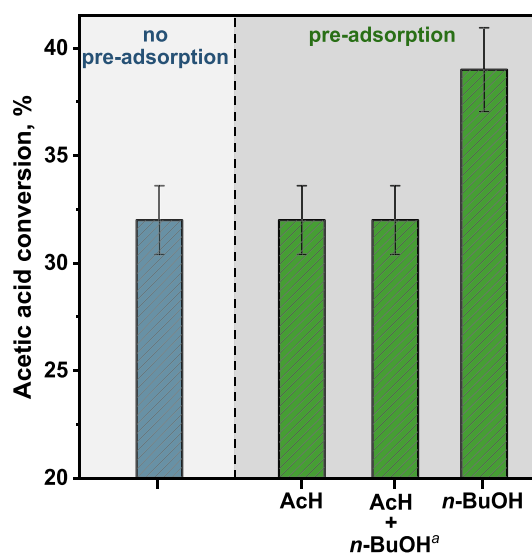

Fig. 6. The effect of reactant pre-adsorption on acetic acid conversion in the esterification of acetic acid with n-butanol in the presence of the sHCP1 catalyst. *Reaction conditions:* AcH (3.84 g, 3.66 mL, 1.0 equiv., 64.0 mmol) or/and n-BuOH (9.49 g, 11.71 mL, 2.0 eqiuv., 128.0 mmol), 20 mg of the sHCP1, 400 rpm, 100 °C, 60 min. [a] calculated by subtracting AcH conversion after 24 h of reaction at room temperature (pre-adsorption of both AcH and n-BuOH only) from AcH conversion after 24 h of pre-adsorption of AcH and n-BuOH at room temperature followed by 60 min of reaction at 100 °C.

the esterification reaction on the surface of sHCPs most probably proceeds according to the Langmuir-Hinshelwood mechanism (see Scheme 2).

In this mechanism, both AcH and n-BuOH are adsorbed and activated on the sHCP-based catalyst most likely by the formation of strong hydrogen bonds between the substrates and the sulfonic acid species of sHCP1 (Scheme 2A) (Miao and Shanks, 2011; Vafaeezadeh and Fattahi, 2015). Subsequently, based on the nature of the nucleophilicity of the alcohol and the electrophilicity of the carbon atom of the carboxylic acid, the adsorbed and non-protonated n-BuOH molecule attacks the carbocation of the adsorbed and protonated AcH molecule (Scheme 2A), producing a tetrahedral intermediate (Scheme 2B) (Zeng et al., 2012). Finally, water is eliminated from the tetrahedral intermediate (Scheme 2C), resulting in the formation of an ester molecule (Scheme 2D). Thus, results obtained during pre-adsorption tests show that the reactivity of sulfonic acid species in esterification may be affected by different hydrophobicity/hydrophilicity of the polymer surface, which determines the efficiency of the alcohol chemisorption. It is very probable that a higher hydrophilicity of the sHCP-based polymer matrix should enable more efficient interaction of the surface active sites with the hydrophilic hydroxyl group of the alcohols, facilitating their more efficient chemisorption and activation. To verify this hypothesis, we compared the hydrophobicity/hydrophilicity of all polymers used in this study on the basis of the data obtained from water contact angle (CA) measurements. As described in our previous work (Wolska et al., 2023), all pristine HCP polymers exhibited slightly hydrophilic surfaces (Table 1). The CA values determined for these materials were similar and ranged from 50 to 58° for HCP1 and HCP3, respectively. After the post-synthetic sulfonation, a significant decrease in CA was observed only for the polymer characterized by the highest cross-linking density (sHCP3). In the case of sHCP1 and sHCP2, the decrease in CA value after post-synthetic sulfonation was less noticeable (Table 1). Based on the above, we claim that the cross-linking density of the polymer matrix affected not only the efficiency of the –SO₃H anchoring but also the localization of these active species. In the case of the material characterized by the lowest cross-linking density (sHCP1), a significant part of all sulfonic acid species was localized inside the pores of the polymer. For this reason,
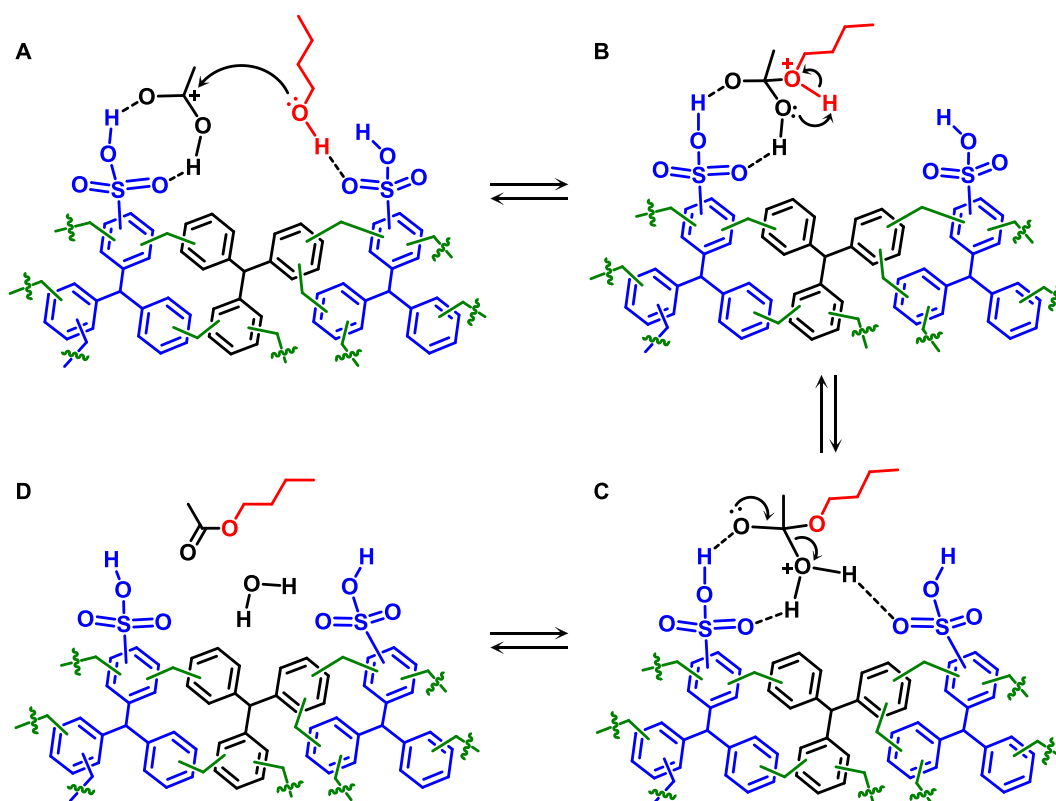
Scheme 2. Possible mechanism for the esterification of acetic acid with *n*-butanol on the surface of the sHCP1 catalyst established on the basis of experimental data.

changes in the CA value of this HCP1 after the post-synthetic sulfonation were negligible (please note that CA is a surface sensitive technique). We also found that the higher cross-linking density of the polymer matrix hindered efficient sulfonation of the polymers inside the pores and promoted more efficient anchoring of –SO₃H species on the external surface. In the polymer characterized by the highest-cross-linking density (sHCP3), the largest part of –SO₃H species was localized on the external surface, resulting in a clearly noticeable decrease in CA value after the post-synthetic sulfonation. For this reason, sHCP3 had the highest hydrophilicity of the polymer surface. Thus, CA measurements confirmed that the highest reactivity of sulfonic acid species anchored on the surface of sHCP3 resulted from the highest hydrophilicity of this material, which facilitated the chemisorption of *n*-butanol on the external surface of the catalyst. Furthermore, CA measurements clearly indicated that the localization of the active sites on the external surface of the polymers and their availability for the reagents are another important factors that promote the high reactivity of the –SO₃H species in esterification.

The hypothesis about important role of the hydrophilicity of the polymer surface in controlling its reactivity in esterification was also confirmed by analyzing TOF values calculated for various alcohols of different relative polarities over sHCP3 (Table 2). Note that the results related to esterification of methanol with acetic acid have not been taken into account because of the totally different reaction temperature. The lowest TOF was observed for the esterification of acetic acid with cyclohexanol, which is the most hydrophobic reagent (Table 2 and Table S3) and its adsorption on sHCP3 should be the lowest due to the highest hydrophilicity of this polymer matrix. In agreement with our hypothesis related to the role of the hydrophilicity of the polymer surface, much higher TOFs were observed for the reactions with the use of benzyl alcohol and *n*-butanol that have comparable relative polarity but significantly higher than that characteristic of cyclohexanol (Table 2 and Table S3). The highest TOF was reported for *n*-BuOH alcohol, as *n*-butanol is more reactive in esterification with AcH than benzyl alcohol

mainly due to the higher bulkiness of BnOH, which may reduce its nucleophilicity (Khan et al., 2021). As far as reactivity of the –SO₃H species on sHCPs is concerned, it is important to underline that relative TOF values calculated for sHCP1, sHCP2 and sHCP3 were clearly affected by the nature and properties of the investigated alcohols (Table S4). The least pronounced differences in the reactivity of the –SO₃H species in the sulfonated polymers were observed for the reaction with the use of the most hydrophilic reagent (methanol). In the case of *n*-butanol, cyclohexanol, and benzyl alcohol, which are known for their lower relative polarity, the differences in relative TOF values were significantly more pronounced (Table S4). In the case of all alcohols used in this work, the highest relative TOF was observed for the most hydrophilic polymer (sHCP3). This further confirms the important role of the polymer hydrophilicity in controlling the reactivity of sulfonic acid species anchored on HCPs in the esterification reaction, and indicates that the highest reactivity of sulfonic acid species in sHCP3 did not result only from the lowest strength of the acid sites in this material. However, the strength of the acid sites and hydrophilicity of the polymers are not the sole factors affecting the reactivity of sulfonic acid species. For example, Amberlyst-15, which has a much higher sulfur loading than the HCPs-based materials used in this work, was far less active both in terms of AcH conversion and reactivity of a single –SO₃H site. This originated most probably from the relatively low surface area of this commercial catalyst, and indicates that high surface area of the polymeric support, ensuring high availability of the active sites to the reagents, also plays an important role in controlling the reactivity of sulfonic acid species anchored on organic polymers.

As far as the reactivity of HCP-based materials in esterification is concerned, it is important to underline that the highest acetic acid conversion was observed for the sHCP1 characterized by the lowest cross-linking density and the highest –SO₃H loading. This clearly shows that the highly efficient HCP-based catalyst dedicated to esterification should exhibit a suitable compromise between the hydrophilicity of the polymer surface as well as localization and loading of sulfonic acid

species in the catalyst.

4. Conclusions

In this study, a series of sulfonated polymers based on HCPs was applied in the esterification of acetic acid with different structure alcohols (methanol, *n*-butanol, cyclohexanol, and benzyl alcohol). It was found that the localization and loading of sulfonic acid species had a significant impact on the hydrophilicity of the polymer surface and the reactivity of the sulfonated catalysts in esterification. Both these parameters are strongly affected by the cross-linking of the polymer matrix. The highest reactivity of sulfonic acid species, expressed as TOF, was observed for the catalyst supported on the polymer characterized by the highest cross-linking density that facilitated more efficient post-synthetic sulfonation of the polymer matrix on its external surface. This resulted in higher hydrophilicity of the catalyst surface in the neighbourhood of sulfonic acid species and enabled more efficient esterification of acetic acid via the Langmuir-Hinshelwood mechanism, in which the rate determining step was the chemisorption of the alcohol. Sulfonic acid species anchored on HCP3 were found to be approximately 7 times more reactive in esterification of acetic acid with *n*-butanol than those of Amberlyst-15 (TOF = 11.36 vs. 1.57 h^{-1}, respectively). As far as the reactivity of the sulfonic acid species is concerned, it is important to underline that the most suitable compromise between the hydrophilicity of the polymer surface and sulfur loading, allowing the highest acetic acid conversion, was observed for the polymer characterized by the lowest cross-linking density (sHCP1). This sulfonated catalyst exhibited approximately two times higher acetic acid conversion in *n*-butanol esterification than Amberlyst-15 (53.6 vs. 27.5 % of AcH conversion) despite of significantly lower loading of the –SO$_3$H groups in the former catalyst (2.22 vs. 4.66 mmol/g, respectively).

The results obtained in this study provide deep insight into the factors affecting the reactivity of sulfonic acid species anchored on hyper-cross-linked polymers in esterification of acetic acid with different structure alcohols. It is expected that this fundamental knowledge may play an important role in the development of novel and more effective solid acid catalysts based on HCPs for the synthesis of organic esters of high industrial significance.

CRediT authorship contribution statement

Joanna Wolska: Conceptualization, Methodology, Validation, Investigation, Resources, Data curation, Writing – original draft, Funding acquisition, Project administration. **Lukasz Wolski:** Methodology, Writing – original draft.

Declaration of competing interest

The authors declare that they have no known competing financial interests or personal relationships that could have appeared to influence the work reported in this paper.

Acknowledgments

Appendix A. Supplementary data

Supplementary data to this article can be found online at https://doi.org/10.1016/j.arabjc.2024.105600.

References

Abbas, A.S., Albayati, T.M., Alismaeel, Z.T., Doyle, A.M., 2016. Kinetics and mass transfer study of oleic acid esterification over prepared nanoporous HY zeolite. Iraqi J Chem. Pet. Eng. 17, 47–60. https://doi.org/10.31699/ijcpe.2016.1.5.

Altıokka, M.R., Çıtak, A., 2003. Kinetics study of esterification of acetic acid with isobutanol in the presence of amberlite catalyst. Appl. Catal. A Gen. 239, 141–148. https://doi.org/10.1016/S0926-860X(02)00381-2.

Ambat, I., Srivastava, V., Sillanpää, M., 2018. Recent advancement in biodiesel production methodologies using various feedstock: A review. Renew. Sustain. Energy Rev. 90, 356–369. https://doi.org/10.1016/j.rser.2018.03.069.

Arca, H.C., Mosquera-Giraldo, L.I., Bi, V., Xu, D., Taylor, L.S., Edgar, K.J., 2018. Pharmaceutical applications of cellulose ethers and cellulose ether esters. Biomacromolecules 19, 2351–2376. https://doi.org/10.1021/acs.biomac.8b00517.

Benessere, V., Cucciolito, M.E., De Santis, A., Di Serio, M., Esposito, R., Melchiorre, M., Nugnes, F., Paduano, L., Ruffo, F., 2019. A sustainable process for the production of varnishes based on pelargonic acid esters. J. Am. Oil Chem. Soc. 96, 443–451. https://doi.org/10.1002/aocs.12200.

Bhorodwaj, S.K., Dutta, D.K., 2011. Activated clay supported heteropoly acid catalysts for esterification of acetic acid with butanol. Appl. Clay Sci. 53, 347–352. https://doi.org/10.1016/j.clay.2011.01.019.

Bhunia, S., Banerjee, B., Bhaumik, A., 2015. A new hypercrosslinked supermicroporous polymer, with scope for sulfonation, and its catalytic potential for the efficient synthesis of biodiesel at room temperature. Chem. Commun. 51, 5020–5023. https://doi.org/10.1039/c4cc09872b.

Blocher, A., Mayer, F., Schweng, P., Tikovits, T.M., Yousefi, N., Woodward, R.T., 2022. One-pot route to fine-tuned hypercrosslinked polymer solid acid catalysts. Mater. Adv. 3, 6335–6342. https://doi.org/10.1039/d2ma00379a.

Bringué, R., Ramírez, E., Iborra, M., Tejero, J., Cunill, F., 2019. Esterification of furfuryl alcohol to butyl levulinate over ion-exchange resins. Fuel 257, 116010. https://doi.org/10.1016/j.fuel.2019.116010.

Desai, D.S., Yadav, G.D., 2023. Synthesis of energy rich fuel additive from biomass derived levulinic acid and furfuryl alcohol using novel tin-exchanged heteropoly acid supported on titania nanotubes as catalyst. Fuel 331, 125700. https://doi.org/10.1016/j.fuel.2022.125700.

Di Menno Di, D., Bucchianico, A., Cipolla, J., Buvat, M., Mignot, V.C., Moreno, S.L., 2022. Kinetic study and model assessment for n-butyl levulinate production from alcoholysis of 5-(hydroxymethyl)furfural over Amberlite IR-120. Ind. Eng. Chem. Res. 61, 10818–10836. https://doi.org/10.1021/acs.iecr.2c01640.

Giri, A., Biswas, S., Hussain, M.W., Dutta, T.K., Patra, A., 2022. Nanostructured hypercrosslinked porous organic polymers: Morphological evolution and rapid separation of polar organic micropollutants. ACS Appl. Mater. Interfaces. 14, 7369–7381. https://doi.org/10.1021/acsami.1c24393.

Gomes, G.J., Zalazar, M.F., Arroyo, P.A., 2022. New insights into the effect of the zeolites framework topology on the esterification reactions: A comparative study from experiments and theoretical calculations. Top. Catal. 65, 871–886. https://doi.org/10.1007/s11244-022-01606-5.

Hamza, M.F., Fouda, A., Elwakeel, K.Z., Wei, Y., Guibal, E., Hamad, N.A., 2021. Phosphorylation of guar gum/magnetite/chitosan nanocomposites for uranium(VI) sorption and antibacterial applications. Molecules 26, 1920. https://doi.org/10.3390/molecules26071920.

He, C., Salih, K.A.M., Wei, Y., Mira, H., Abdel-Rahman, A.A.H., Elwakeel, K.Z., Hamza, M.F., Guibal, E., 2021. Efficient recovery of rare earth elements (Pr(III) and Tm(III)) from mining residues using a new phosphorylated hydrogel (Algal Biomass/PEI). Metals 11, 1–29. https://doi.org/10.3390/met11020294.

Healy, C., Patil, K.M., Wilson, B.H., Hermanspahn, L., Harvey-reid, N.C., Howard, B.I., Kleinjan, C., Kolien, J., Payet, F., Telfer, S.G., Kruger, P.E., Bennett, T.D., 2020. The thermal stability of metal-organic frameworks. Coord. Chem. Rev. 419, 213388 https://doi.org/10.1016/j.ccr.2020.213388.

Hosseini, M.S., Masteri-Farahani, M., 2019. Surface functionalization of magnetite nanoparticles with sulfonic acid and heteropoly acid: Efficient magnetically recoverable solid acid catalysts. Chem. - an Asian J. 14, 1076–1083. https://doi.org/10.1002/asia.201801810.

https://www.futuremarketinsights.com/reports/esters-market.

Hu, X., Ma, K., Sabbaghi, A., Chen, X., Chatterjee, A., Lam, F.L.Y., 2020. Mild acid functionalization of metal-organic framework and its catalytic effect on esterification of acetic acid with n-butanol. Mol. Catal. 482, 110635 https://doi.org/10.1016/j.mcat.2019.110635.

Hykkerud, A., Marchetti, J.M., 2016. Esterification of oleic acid with ethanol in the presence of Amberlyst 15. Biomass Bioenergy 95, 340–343. https://doi.org/10.1016/j.biombioe.2016.07.002.

Kalla, R.M.N., Kim, M.-R., Kim, I., 2018. Sulfonic acid-functionalized, hyper-cross-linked porous polyphenols as recyclable solid acid catalysts for esterification and transesterification reactions. Ind. Eng. Chem. Res. 57, 11583–11591. https://doi.org/10.1021/acs.iecr.8b02418.

Khan, Z., Javed, F., Shamair, Z., Hafeez, A., Fazal, T., Aslam, A., Zimmerman, W.B., Rehman, F., 2021. Current developments in esterification reaction: A review on process and parameters. J. Ind. Eng. Chem. 103, 80–101. https://doi.org/10.1016/j.jiec.2021.07.018.

Khan, N.R., Rathod, V.K., 2015. Enzyme catalyzed synthesis of cosmetic esters and its intensification: A review. Process Biochem. 50, 1793–1806. https://doi.org/10.1016/j.procbio.2015.07.014.

Kim, H., Yang, S., Kim, D.H., 2020. One-pot conversion of alginic acid into furfural using Amberlyst-15 as a solid acid catalyst in γ-butyrolactone/water co-solvent system. Environ. Res. 187, 109667 https://doi.org/10.1016/j.envres.2020.109667.

Kundu, S.K., Bhaumik, A., 2015. Pyrene-based porous organic polymers as efficient catalytic support for the synthesis of biodiesels at room temperature. ACS Sustain. Chem. Eng. 3, 1715–1723. https://doi.org/10.1021/acssuschemeng.5b00238.

Lee, M.-J., Chiu, J.-Y., Lin, H., 2002. Kinetics of catalytic esterification of propionic acid and n-butanol over amberlyst 35. Ind. Eng. Chem. Res. 41, 2882–2887. https://doi.org/10.1021/ie0105472.

Li, B., Gong, R., Wang, W., Huang, X., Zhang, W., Li, H., Hu, C., Tan, B., 2011. A new strategy to microporous polymers: Knitting rigid aromatic building blocks by external cross-linker. Macromolecules 44, 2410–2414. https://doi.org/10.1021/ma200630s.

Li, H., Zhao, S., Zhang, W., Du, H., Yang, X., Peng, Y., Han, D., Wang, B., Li, Z., 2023. Efficient esterification over hierarchical Zr-Beta zeolite synthesized via liquid-state ion-exchange strategy. Fuel 342, 127786. https://doi.org/10.1016/j.fuel.2023.127786.

Liu, Y., Lotero, E., Goodwin Jr., J.G., 2006. Effect of water on sulfuric acid catalyzed esterification. J. Mol. Catal. A Chem. 245, 132–140. https://doi.org/10.1016/j.molcata.2005.09.049.

Liu, Y., Lotero, E., Goodwin Jr., J., 2006. A comparison of the esterification of acetic acid with methanol using heterogeneous versus homogeneous acid catalysis. J. Catal. 242, 278–286. https://doi.org/10.1016/j.jcat.2006.05.026.

Liu, X., Wang, C., Zhou, J., Liu, C., Liu, Z., Shi, J., Wang, Y., Teng, J., Xie, Z., 2022. Molecular transport in zeolite catalysts: depicting an integrated picture from macroscopic to microscopic scales. Chem. Soc. Rev. 51, 8174–8200. https://doi.org/10.1039/D2CS00079B.

Manjunathan, P., Upare, P.P., Lee, M., Hwang, D.W., 2021. One-pot fructose conversion into 5-ethoxymethylfurfural using a sulfonated hydrophobic mesoporous organic polymer as a highly active and stable heterogeneous catalyst. Catal Sci. Technol. 11, 5816–5826. https://doi.org/10.1039/d1cy00883h.

Masteri-Farahani, M., Shahsavarifar, S., 2021. Chemical functionalization of chitosan biopolymer and chitosan-magnetite nanocomposite with sulfonic acid for acid-catalyzed reactions, Chinese. J Chem. Eng. 39, 154–161. https://doi.org/10.1016/j.cjche.2021.04.037.

Melfi, D.T., dos Santos, K.C., Ramos, L.P., Corazza, M.L., 2020. Supercritical CO₂ as solvent for fatty acids esterification with ethanol catalyzed by Amberlyst-15. J. Supercrit. Fluids. 158, 104736. https://doi.org/10.1016/j.supflu.2019.104736.

Miao, S., Shanks, B.H., 2011. Mechanism of acetic acid esterification over sulfonic acid-functionalized mesoporous silica. J. Catal. 279, 136–143. https://doi.org/10.1016/j.jcat.2011.01.008.

Mirabedini, S.M., Zareanshahraki, F., Mannari, V., 2020. Enhancing thermoplastic road-marking paints performance using sustainable rosin ester. Prog. Org. Coatings. 139, 105454 https://doi.org/10.1016/j.porgcoat.2019.105454.

Mitran, G., Yuzhakova, T., Popescu, I., Marcu, I.C., 2015. Study of the esterification reaction of acetic acid with n-butanol over supported WO₃ catalysts. J. Mol. Catal. A Chem. 396, 275–281. https://doi.org/10.1016/j.molcata.2014.10.014.

Mohamed, E.A., Betiha, M.A., Negm, N.A., 2023. Insight into the recent advances in sustainable biodiesel production by catalytic conversion of vegetable oils: Current trends, challenges, and prospects. Energy Fuel 37, 2631–2647. https://doi.org/10.1021/acs.energyfuels.2c03887.

Munyentwali, A., Li, C., Li, H., Yang, Q., 2021. Synthesis of sulfonated porous organic polymers with a hydrophobic core for efficient acidic catalysis in organic transformations. Chem. - an Asian J. 16, 2041–2047. https://doi.org/10.1002/asia.202100456.

Paiva, M.F., de Freitas, E.F., Campos de França, J.O., da Silva Valadares, D., Loureiro Dias, S.C., Alves Dias, J., 2022. Structural and acidity analysis of heteropolyacids supported on faujasite zeolite and its effect in the esterification of oleic acid and n-butanol. Mol. Catal. 532, 112737 https://doi.org/10.1016/j.mcat.2022.112737.

Pan, H., Wang, J., Chen, L., Su, G., Cui, J., Meng, D., Wu, X., 2013. Preparation of sulfated alumina supported on mesoporous MCM-41 silica and its application in esterification. Catal. Commun. 35, 27–31. https://doi.org/10.1016/j.catcom.2013.02.007.

Paul, G., Begni, F., Melicchio, A., Golemme, G., Bisio, C., Marchi, D., Cossi, M., Marchese, L., Gatti, G., 2020. Hyper-cross-linked polymers for the capture of aromatic volatile compounds. ACS Appl. Polym. Mater. 2, 647–658. https://doi.org/10.1021/acsapm.9b01000.

Pirez, C., Caderon, J.M., Dacquin, J.P., Lee, A.F., Wilson, K., 2012. Tunable KIT-6 mesoporous sulfonic acid catalysts for fatty acid esterification. ACS Catal. 2, 1607–1614. https://doi.org/10.1021/cs300161a.

Pöpken, T., Steinigeweg, S., Gmehling, J., 2001. Synthesis and hydrolysis of methyl acetate by reactive distillation using structured catalytic packings: Experiments and simulation. Ind. Eng. Chem. Res. 40, 1566–1574. https://doi.org/10.1021/ie0007419.

Prinsen, P., Luque, R., González-Arellano, C., 2018. Zeolite catalyzed palmitic acid esterification. Microporous Mesoporous Mater. 262, 133–139. https://doi.org/10.1016/j.micromeso.2017.11.029.

Reinoso, D.M., Boldrini, D.E., 2020. Kinetic study of fuel bio-additive synthesis from glycerol esterification with acetic acid over acid polymeric resin as catalyst. Fuel 264, 116879. https://doi.org/10.1016/j.fuel.2019.116879.

Sá, A.G.A., de Meneses, A.C., de Araújo, P.H.H., de Oliveira, D., 2017. A review on enzymatic synthesis of aromatic esters used as flavor ingredients for food, cosmetics and pharmaceuticals industries. Trends Food Sci. Technol. 69, 95–105. https://doi.org/10.1016/j.tifs.2017.09.004.

Taddeo, F., Vitiello, R., Tesser, R., Melchiorre, M., Eränen, K., Salmi, T., Russo, V., Di Serio, M., 2022. Nonanoic acid esterification with 2-ethylhexanol: From batch to continuous operation. Chem. Eng. J. 444, 136572 https://doi.org/10.1016/j.cej.2022.136572.

Tan, L., Tan, B., 2017. Hypercrosslinked porous polymer materials: Design, synthesis, and applications. Chem. Soc. Rev. 46, 3322–3356. https://doi.org/10.1039/c6cs00851h.

Vafaeezadeh, M., Fattahi, A., 2015. DFT investigations for "Fischer" esterification mechanism over silica-propyl-SO₃H catalyst: Is the reaction reversible? Comput. Theor. Chem. 1071, 27–32. https://doi.org/10.1016/j.comptc.2015.07.028.

Wang, W., Qin, C., Li, W., Ge, J., Feng, C., 2020. Improving moisture barrier properties of paper sheets by cellulose stearoyl ester-based coatings. Carbohydr. Polym. 235, 115924 https://doi.org/10.1016/j.carbpol.2020.115924.

Wei, Y., Salih, K.A.M., Rabie, K., Elwakeel, K.Z., Zayed, Y.E., Hamza, M.F., Guibal, E., 2021. Development of phosphoryl-functionalized algal-PEI beads for the sorption of Nd(III) and Mo(VI) from aqueous solutions – Application for rare earth recovery from acid leachates. Chem. Eng. J. 412, 127399 https://doi.org/10.1016/j.cej.2020.127399.

Wolska, J., Stawicka, K., Walkowiak-Kulikowska, J., 2021. Sulfonic-acid-functionalized polymers based on fluorinated methylstyrenes and styrene as promising heterogeneous catalysts for esterification. Mater. Chem. Phys. 273, 125132 https://doi.org/10.1016/j.matchemphys.2021.125132.

Wolska, J., Muńko, M., EL Siblani, H., Telegeiev, I., Frankowski, M., Szwajca, A., Walkowiak-Kulikowska, J., El-Roz, M., Wolski, L., 2023. The influence of cross-linking density on the efficiency of post-synthetic sulfonation of hyper-cross-linked polymers and their adsorption capacity for antibiotic pollutants. J. Environ. Chem. Eng. 11, 110429 https://doi.org/10.1016/j.jece.2023.110429.

Woodward, R.T., 2020. The design of hypercrosslinked polymers from benzyl ether self-condensing compounds and external crosslinkers. Chem. Commun. 56, 4938–4941. https://doi.org/10.1039/D0CC01002B.

Yahya, R., Elshaarawy, R.F.M., 2023. Highly sulfonated chitosan-polyethersulfone mixed matrix membrane as an effective catalytic reactor for esterification of acetic acid. Catal. Commun. 173, 106557 https://doi.org/10.1016/j.catcom.2022.106557.

Yılmaz, E., Sert, E., Atalay, F.S., 2017. Synthesis and sulfation of titanium based metal organic framework; MIL-125 and usage as catalyst in esterification reactions. Catal. Commun. 100, 48–51. https://doi.org/10.1016/j.catcom.2017.06.026.

Zang, Y., Shi, J., Zhang, F., Zhong, Y., Zhu, W., 2013. Sulfonic acid-functionalized MIL-101 as a highly recyclable catalyst for esterification. Catal Sci. Technol. 3, 2044–2049. https://doi.org/10.1039/c3cy00044c.

Zeng, Z., Cui, L., Xue, W., Chen, J., Che, Y., 2012. Recent developments on the Mechanism and kinetics of esterification reaction promoted by various catalysts. in: Chem. Kinet., InTech 255–282. https://doi.org/10.5772/38106.

Zhang, X., Zhao, Y., Yang, Q., 2014. PS-SO₃H@phenylenesilica with yolk–double-shell nanostructures as efficient and stable solid acid catalysts. J. Catal. 320, 180–188. https://doi.org/10.1016/j.jcat.2014.09.018.

Zhang, C., Zhuang, Q., Wang, H., Ying, X., Ji, R., Sheng, D., Dong, W., Xie, A., 2023. Constructing an acidic microenvironment by sulfonated polymers for photocatalytic reduction of hexavalent chromium under neutral conditions. J. Colloid Interface Sci. 630, 235–248. https://doi.org/10.1016/j.jcis.2022.10.055.

Zhao, X., Wang, Q., Kunthom, R., Liu, H., 2023. Sulfonic acid-grafted hybrid porous polymer based on double-decker silsesquioxane as highly efficient acidic heterogeneous catalysts for the alcoholysis of styrene oxide. ACS Appl. Mater. Interfaces. 15, 6657–6665. https://doi.org/10.1021/acsami.2c17732.

Zheng, M.M., Lu, Y., Huang, F.H., Wang, L., Guo, P.M., Feng, Y.Q., Deng, Q.C., 2013. Lipase immobilization on hyper-cross-linked polymer-coated silica for biocatalytic synthesis of phytosterol esters with controllable fatty acid composition. J. Agric. Food Chem. 61, 231–237. https://doi.org/10.1021/jf3042962.